NASA TECHNICAL MEMORANDUM

NASA TM X-73497

NASA TM X-73497

(NASA-TM-X-73497) COMPENSATED CONTROL LOOPS FOR A 30-cm ION THRUSTER (NASA) 17 p HC A02/MF A01 CSCL 21C

N77-11100

Unclas

G3/20 54473

COMPENSATED CONTROL LOOPS FOR A 30-CM ION THRUSTER

by R. R. Robson
Lewis Research Center
Cleveland, Ohio 44135

TECHNICAL PAPER to be presented at the
Twelfth International Electric Propulsion Conference sponsored by the
American Institute of Aeronautics and Astronautics
Key Biscayne, Florida, November 15-17, 1976

COMPENSATED CONTROL LOOPS FOR A 30-CM ION THRUSTER

R. R. Robson
National Aeronautics and Space Administration
Lewis Research Center
Cleveland, Ohio

E-8895

Abstract

The vaporizer dynamic control characteristics of a 30-cm diameter mercury ion thruster were determined by operating the thruster in an open loop steady state mode and then introducing a small sinusoidal signal on the main, cathode, or neutralizer vaporizer current and observing the response of the beam current, discharge voltage, and neutralizer keeper voltage, respectively. This was done over a range of frequencies and operating conditions. From these data, Bode plots for gain and phase were made and mathematical models were obtained. The Bode plots and mathematical models were analyzed for stability and appropriate compensation networks determined. The compensated control loops were incorporated into a power processor and operated with a thruster. The time responses of the compensated loops to changes in set points and recovery from arc conditions are presented.

Introduction

The long term stable operation of 30-cm diameter mercury ion thrusters(1) requires that the beam current, discharge voltage, and neutralizer keeper voltage be maintained within less than one percent of their setpoints to achieve proposed mission goals. These parameters are controlled by the mercury vapor flow through the main vaporizer, the cathode vaporizer, and the neutralizer vaporizer, respectively. The mercury vapor flow rate through a porous tungsten vaporizer is a function of the temperature of the porous plug which is controlled by the current through its heater. Therefore, to automatically control the beam current, the discharge voltage and the neutralizer keeper voltage at their setpoint values, the current in their respective vaporizer heaters must be closed loop controlled.

In the past, this control has been implemented with noncompensated proportional control loops. This approach does not allow sufficient open loop gain to maintain the controlled parameters within ±1% while maintaining stability. It also results in a nonlinear relationship between the reference signal and the controlled parameter due to the nonlinear relationship between the vaporizer heater current and the controlled parameter. This nonlinearity is undesirable for computer control of the thruster. Therefore, a control philosophy is required that will provide an open loop gain of greater than 100 to maintain the controlled parameters within less than ±1% and will linearize the relationships between the reference signals and the controlled parameters.

The approach adopted was to use an integrator in the control loop. This results in infinite d.c. open loop gain and linearizes the relationship between the reference signal and the controlled parameter. The control loop is then compensated to provide a stable system over a 4 to 1 thrust range and a simulated thruster thermal environment of 0 to 2 suns.

The time response of the control loops is equally important. The thruster should respond to changes in setpoints in less than 60 seconds and return to a steady state operating point from an arc condition in less than 15 seconds. An additional requirement is that the beam current must not overshoot its setpoint by more than 1% to prevent possible collapse of the solar array voltage on a spacecraft.

Compensated control loops also eliminate the need for fine tuning the control loops in a power processor to a given thruster. The compensation is achieved for the range of thruster characteristics that normally exists from one thruster to another.

The assistance of Mr. James Budinger in obtaining this data is greatly appreciated.

Apparatus

The thruster tests were performed in the 3.05 m bell jar of the 7.6 m diameter vacuum facility[2] at Lewis Research Center. The power supply system used to operate the thruster for these tests was an inverter type laboratory system.[3] The thruster tested was Engineering Model Thruster (EMT) serial number 802. The 0 and 2 solar constant (sun) thermal environment was provided by a heated cylindrical shield placed around the thruster. This shield was used to heat the ground screen and back plate of the thruster to temperatures representative of two suns. These temperatures were determined in thermal tests using an arc lamp solar simulator source.[4]

Procedure

The thruster was operated at selected points in an open loop mode and allowed to reach thermal equilibrium. The cathode and neutralizer vaporizer currents were held constant, and a small sinusoidal signal was introduced on the main vaporizer current. The subsequent response of the beam current and discharge voltage were recorded on a strip chart recorder, along with the main vaporizer current. The responses were recorded for a number of frequencies between 0.001 and 0.1 Hz. The main and neutralizer vaporizer currents were then held constant, and the sinusoidal signal introduced on the cathode vaporizer current. The response of the beam current, and discharge voltage were recorded along with the cathode vaporizer current. Finally the main and cathode vaporizers were operated at a fixed current and the sinusoidal signal introduced on the neutralizer vaporizer current. The response of the neutralizer keeper voltage was recorded along with the neutralizer vaporizer current.

The above procedure was followed for operating points of full, one-half, and one-fourth thrust and for solar thermal environments of zero and two suns. Bode plots were made from these data and the control loops analyzed for stability. Integrators and lead networks were then added to the control loops of the power processor and the gains of the loops adjusted

STAR Category 20

to provide the desired time responses with the thruster.

Results and Discussion

Frequency Responses

The Bode plots for beam current (J_B) versus main vaporizer current (J_V), and discharge voltage (ΔV_I) versus main vaporizer current (J_V) at beam currents of 2, 1, and 0.5 amperes are shown in Figure 1 for the zero sun condition. These beam currents represent thrust levels of full, one-half, and one-fourth thrust, respectively.

The thruster operating conditions for all data taken are shown in Table 1.

The Laplace transfer functions, in the s domain, derived from these Bode plots are:

$$\frac{J_B}{J_V} = \frac{K}{\left(\frac{s}{0.01} + 1\right)\left(\frac{s}{2} + 1\right)}$$

where $K = 2.4$ for 2 amperes, 1.9 for 1 ampere, and 0.7 for 0.5 ampere and

$$\frac{\Delta V_I}{J_V} = \frac{-K}{\left(\frac{s}{0.01} + 1\right)\left(\frac{s}{2} + 1\right)}$$

where $K = 50$ for 2 amperes, 11 for 1 ampere, and 18 for 0.5 ampere (Table 2).

Except for the gain term K, both transfer functions are identical for all three beam currents with break frequencies at $\omega = 0.01$ radians/sec and $\omega = 2$ radians/sec.

The Bode plots for J_B versus J_V and ΔV_I versus J_V at 2 suns are shown in Figure 2.

The transfer functions derived from these Bode plots are:

$$\frac{J_B}{J_V} = \frac{K}{\left(\frac{s}{0.01} + 1\right)\left(\frac{s}{2} + 1\right)}$$

where $K = 2.8$ for 2 amperes and 1.6 for 1 ampere and

$$\frac{\Delta V_I}{J_V} = \frac{-K}{\left(\frac{s}{0.01} + 1\right)\left(\frac{s}{2} + 1\right)}$$

where $K = 28$ for 2 amperes and 18 for 1 ampere.

Again, except for the gain term K, both transfer functions are identical for both beam currents and are identical with the zero sun transfer functions. Therefore, gain is the only parameter that changes as operating-conditions change with the break frequencies remaining constant. Therefore, in compensating the control loop, gain change is the only parameter that needs to be taken into account.

The Bode plots for discharge voltage (ΔV_I) versus cathode vaporizer current (J_{CV}) and beam current (J_B) versus cathode vaporizer current (J_{CV}) for 2, 1, and 0.5 amperes beam currents at zero sun are shown in Figure 3.

The transfer functions derived from these Bode plots are:

$$\frac{\Delta V_I}{J_{CV}} = \frac{-K}{\left(\frac{s}{0.03} + 1\right)\left(\frac{s}{0.5} + 1\right)}$$

where $K = 32$ for 2 amperes, 40 for 1 ampere, and 14 for 0.5 ampere and

$$\frac{J_B}{J_{CV}} = \frac{-K}{\left(\frac{s}{0.03} + 1\right)\left(\frac{s}{0.5} + 1\right)}$$

where $K = 1.3$ for 2 amperes, 0.35 for 1 ampere, and 0.18 for 0.5 ampere.

The Bode plots for ΔV_I versus J_{CV} and J_B versus J_{CV} at 2 suns are shown in Figure 4.

The transfer functions derived from these Bode plots are:

$$\frac{\Delta V_I}{J_{CV}} = \frac{-K}{\left(\frac{s}{0.03} + 1\right)\left(\frac{s}{0.5} + 1\right)}$$

where $K = 56$ for 2 amperes and 22 for 1 ampere and

$$\frac{J_B}{J_{CV}} = \frac{-K}{\left(\frac{s}{0.03} + 1\right)\left(\frac{s}{0.5} + 1\right)}$$

where $K = 0.89$ for 2 amperes and 0.45 for 1 ampere.

As in the case of the main vaporizer, the break frequencies for the cathode vaporizer remain fixed and gain is the only parameter that changes. The break frequencies for the cathode vaporizer occur at $\omega = 0.03$ radians/sec and $\omega = 0.5$ radians/sec.

The Bode plots for neutralizer keeper voltage (V_{NK}) versus neutralizer vaporizer current (J_{NV}) for 2, 1, 0.5, and 0.0 ampere beam currents at zero sun are shown in Figure 5. The transfer function derived from these Bode plots is:

$$\frac{V_{NK}}{J_{NV}} = \frac{-K}{\left(\frac{s}{0.02} + 1\right)\left(\frac{s}{2} + 1\right)}$$

where $K = 10.0$ for 2 amperes, 7.1 for 1 ampere, 44.8 for 0.5 ampere, and 12.5 for 0.0 ampere.

The Bode plots for 2 suns are shown in Figure 6. The transfer function derived from these Bode plots is:

$$\frac{V_{NK}}{J_{NV}} = \frac{-K}{\left(\frac{s}{0.02} + 1\right)\left(\frac{s}{2} + 1\right)}$$

where $K = 14$ for 2 amperes and 50 for 1 ampere.

As in the cases of the other two vaporizers, the break frequencies for the neutralizer vaporizer remain fixed and gain is the only variable. The break frequencies for the neutralizer vaporizer occur at $\omega = 0.02$ radians/sec and $\omega = 2$ radians/sec.

From the Bode plots for these transfer functions it can be determined that the maximum open loop gains permissible to maintain a minimum 60° phase margin, using straight proportional control are:

Main vaporizer loop	39 dB
Cathode vaporizer loop	17.5 dB
Neutralizer vaporizer loop	34 dB

However, these gains are not sufficient to maintain J_B, ΔV_I, and V_{NK} within 1% of their set points under all conditions.

The interactions of the main vaporizer and the cathode vaporizer on J_B and ΔV_I can also be seen from these Bode plots. Although J_{CV} is the primary control for ΔV_I, the $\Delta V_I/J_V$ transfer function under some conditions has a higher gain than the $\Delta V_I/J_{CV}$ transfer function (Table 2). The cathode vaporizer also has a strong effect on the beam current. This strong interaction between the two loops could lead to instabilities.

Compensated Loops

Figure 7 shows the straight line approximation Bode plots for the compensated loop of J_B/J_V. The transfer function for this compensated loop is:

$$\frac{J_B}{J_V} = \frac{7.5\left(\frac{s}{0.05}+1\right)\left(\frac{s}{8}+1\right)}{s\left(\frac{s}{0.01}+1\right)\left(\frac{s}{2}+1\right)}$$

The control loop that was implemented into the power processor is shown in Figure 8. This compensated loop contains an integrator to provide infinite d.c. gain and to linearize the relationship between the reference signal and the J_B signal. This integrator passes through 0.0 dB at $\omega = 1.0$ radians/sec. The loop also contains two lead networks to maintain 60° of phase margin out to $\omega = 5$ radians/sec minimum. One lead is at $\omega = 0.05$ radians/sec and the other one is at $\omega = 8.0$ radians/sec. The open loop gain at $\omega = 1.0$ radians/sec is 4 dB.

The output of the integrator is limited in both the positive and negative directions to the minimum values needed to provide a steady state J_V range of 0.0 to 2.0 amperes. This is done to prevent the integrator from running away during off normal conditions. If the integrator is not limited, large overshoots occur when recovering from these off-normal conditions.

The straight line approximation Bode plots for the compensated loop of $\Delta V_I/J_{CV}$ are shown in Figure 9. The transfer function for this loop is:

$$\frac{\Delta V_I}{J_{CV}} = \frac{-1.9\left(\frac{s}{0.15}+1\right)\left(\frac{s}{0.5}+1\right)}{s\left(\frac{s}{0.03}+1\right)\left(\frac{s}{0.5}+1\right)}$$

Figure 10 shows the control loop that was implemented into the power processor. This loop, like the J_B/J_V loop contains an integrator and two lead networks. The integrator passes through 0.0 dB at $\omega = 1.0$ radian/sec and the two lead networks are at $\omega = 0.15$ radian/sec and $\omega = 0.5$ radian/sec. This provides 60° of phase margin out past $\omega = 5$ radians/sec. The open loop gain at $\omega = 1.0$ radian/sec is -10 dB.

Figure 11 shows the Bode plots for the compensated loop of V_{NK}/J_{NV}. The transfer function for this loop is:

$$\frac{V_{NK}}{J_{NV}} = \frac{-8.2\left(\frac{s}{0.1}+1\right)\left(\frac{s}{10}+1\right)}{s\left(\frac{s}{0.02}+1\right)\left(\frac{s}{2}+1\right)}$$

Figure 12 shows the control loop that was implemented into the power processor. This loop like the other compensated loops contains an integrator and two lead networks. The integrator passes through 0.0 dB at $\omega = 1.0$ radian/sec and the two leads are at $\omega = 0.1$ radian/sec and $\omega = 10.0$ radians/sec. This provides 60° of phase margin out past $\omega = 5.0$ radians/sec. The open loop gain at $\omega = 1.0$ radian/sec is 4 dB.

Time Responses

Figure 13 shows the time responses of J_B and ΔV_I in throttling from a beam current of 1.8 to 1.9 to 2.0 to 1.9 to 1.8 amperes. In throttling to higher J_B (up), J_B reaches steady state within 15 seconds with less than 1% overshoot. ΔV_I immediately increases to 37.5 volts due to the step change increase in emission current (J_E), and returns to 36 volts within 20 seconds. In throttling to lower current (down), J_B reaches steady state within 10 seconds with no noticeable undershoot. ΔV_I immediately decreases to 35 volts due to the step change decrease in J_E, and returns to 36 volts within 20 seconds.

The time responses of J_B and ΔV_I in throttling from 1.0 to 1.1 amperes and back to 1.0 ampere are shown in Figure 14. In throttling up, J_B reaches steady state within 15 seconds with approximately 1% overshoot. ΔV_I immediately increases to 38 volts due to the step change increase in J_E, and returns to 36 volts within 30 seconds. In throttling down, J_B reaches steady state within 20 seconds with no undershoot. ΔV_I immediately decreases to approximately 34.5 volts due to the step change decrease in J_E, and returns to 36 volts within 20 seconds. It takes longer to throttle down at a beam current of 1 ampere than it does at a beam current of 2 amperes due to the slower cool down of the main vaporizer at 1 ampere.

Figure 15 shows the time responses of J_B and ΔV_I in throttling from a beam current of 0.5 to 0.6 ampere and back to 0.5 ampere. In throttling up J_B reaches steady state within 30 seconds and does not overshoot. ΔV_I shifted its operating point at 0.5 ampere to approximately 35 volts due to the effects of a very noisy ΔV_I signal on the control loop. The thruster operated in a very noisy mode at this beam current level. ΔV_I immediately increased to 38 volts due to the step change increase in J_E for throttling up. It then settled out at the 35 volt operating point within 50 seconds. In throttling down, J_B reaches steady

ORIGINAL PAGE IS
OF POOR QUALITY

state with a 40 seconds and does not undershoot. ΔV_I immediately decreases to 32 5 volts due to the step change decrease in J_E, and returns to 35 volts within 50 seconds. The longer throttle up time at this current level is due to the lower gain in the thruster of the J_B/J_V transfer function.

There does not appear to be any instabilities in these two loops caused by the loops themselves or by the strong interaction that exists between them.

Throttling of the thruster had no noticeable effect on V_{NK}.

The responses of J_B and ΔV_I to a high voltage recycle of the thruster at a beam current of 2 amperes are shown in Figure 16. When the high voltages turn off and J_B goes to zero, J_E is automatically cut back to less than 4 amperes. This causes the immediate drop in voltage of ΔV_I. When the high voltages are turned back on and J_E increases up to its 11.0 amperes set point, ΔV_I overshoots its 36 volt set point and goes to 40 volts. J_B also increases as J_E rises and overshoots its 2 amperes setpoint by 5% due to the overshoot of ΔV_I. Both loops then settle out to their set points within 25 seconds. There is no way to prevent the overshoot of J_B by control of the main vaporizer if ΔV_I overshoots and there is no way to prevent the overshoot of ΔV_I by control of the cathode vaporizer. The prevention of the overshoot of ΔV_I is a function of the recycle sequence. The power processor being used did not have a proper sequence to prevent this overshoot.

Figure 17 shows the responses of J_B and ΔV_I to a recycle of the thruster at a beam current of 1 ampere and Figure 18 shows their responses to a recycle of the thruster at a beam current of 0.5 ampere. The responses are similar to the 2 ampere case except the overshoots of ΔV_I and J_B are smaller.

Figure 19 shows the response of V_{NK} to a recycle of the thruster at a beam current of 2 amperes. When the high voltages are turned off and the beam current goes to zero, the neutralizer keeper current (J_{NK}) is automatically increased from 1.8 to 2.4 amperes and this causes V_{NK} to increase. After the high voltages have been turned back on and the beam current established, J_{NK} is reduced from 2.4 amperes back to its setpoint of 1.8 amperes. This causes V_{NK} to decrease and settle out at its setpoint within 15 seconds.

The response of V_{NK} to recycles of the thruster at beam currents of 1.0 and 0.5 ampere are shown by Figures 20 and 21, respectively. The 1 ampere case is similar to the 2.0 ampere case. At 0.5 ampere, the neutralizer discharge was extinguishing during the recycle and then reigniting after the beam current was established again. This is not normal and is believed to have been caused by the output impedance of the neutralizer keeper power supply being capacitive rather than inductive. Once the neutralizer was reestablished, the control loop returned V_{NK} to its set point.

Conclusion

The dynamic vaporizer control characteristics of a 30-cm diameter mercury ion thruster were obtained. This was accomplished by operating the thruster in an open loop steady state mode and then introducing a small sinusoidal signal on the main, cathode, or neutralizer vaporizer current and observing the response of the beam current, discharge voltage, and neutralizer keeper voltage, respectively. Bode plots were made from this data and transfer functions of the thruster determined from the Bode plots.

The relationships between the controlled parameters and their reference signals were linearized by adding integrators to the control loops. The integrators also provide infinite d.c. gain to hold the parameters within 1% of their respective setpoints over a 25 to 100% thrust range and a solar thermal environment of 0 to 2 suns. Two lead networks were added to each of the control loops. These provide stability, and allow for sufficient gain to keep the time responses, to changes in operating conditions, less than 60 seconds. The beam current overshoots its setpoint by less than 1% during throttling, but by 5% in return to steady state after an arc condition. This 5% is a function of the recycle sequence used on this particular power processor and can be eliminated with a proper recycle sequence. If the beam current overshoots its setpoint by more than 1%, the solar array on a spacecraft may collapse.

These compensated control loops provide a stable low drift control for an ion thruster. They also eliminate the need for fine tuning the control loops in a power processor to a particular thruster. This is accomplished by the compensated control loop's ability to cover the narrow range of thruster characteristics that normally exists from one thruster to another.

References

1. Sovey, J. S. and King, H. J., "Status of 30 Centimeter Mercury Ion Thruster Development," Paper No. 74-1117, AIAA/SAE, 10th Propulsion Conference, San Diego, Calif., Oct. 21-23, 1974.
2. Finke, R. C., Homes, A. D., and Keller, T. A., "Space Environment Facility for Electric Propulsion Systems Research," TN D-2774, 1965, NASA.
3. Terdan, F. F. and Bechtel, R. T., "Control of a 30-cm-Diameter Mercury Bombardment Thruster," Paper No. 73-1079, AIAA 10th Electric Propulsion Conference Lake Tahoe, Nev., Oct. 31-Nov. 2, 1973.
4. Mirtich, M. J., "Thermal-Environment Testing of a 30-cm Engineering Model Thruster," to be presented at AIAA International 12th Electric Propulsion Conference, Key Biscayne, Fla., Nov. 15-17, 1976.

ORIGINAL PAGE IS OF POOR QUALITY

Table 1 Thruster nominal (±3%) operating conditions for all data taken

Beam current, J_B, A	Thermal input, sun	Screen voltage, V_I, V	Accelerator voltage, V_A, V	Discharge voltage, ΔV_I, V	Emission current, J_E, A	Magnetic baffle current, J_{MB}, A	Neutralizer keeper voltage, V_{NK}, V	Neutralizer keeper current, J_{NK}, A
2	0	1100	-390	36.2	10.96	2.2	13.3	1.81
1	0	1100	-400	35.9	5.53	2.4	13.5	1.83
0.5	0	1100	-390	36.0	2.74	1.3	15.4	1.82
0.0	0	0	0	36.0	10.4	2.2	14.0	2.4
2	2	1100	-390	35.9	11.02	2.2	14.0	1.80
1	2	1100	-380	36.2	5.50	2.4	15.0	1.83

Table 1 Continued

Coupling voltage, V_G, V	Main vaporizer temp., T_V, °C	Cathode vaporizer temp., T_{CV}, °C	Neutralizer vaporizer temp., T_{NV}, °C	Ground screen temp., °C	Back plate temp., °C
-11.3	275	322	289	123	144
-11.0	250	332	281	95	111
-10.4	(a)	324	280	(a)	(a)
(b)	220	344	288	(a)	(a)
-11.7	294	340	330	217	210
-11.5	265	340	300	197	185

[a]Data not available.

[b]Data does not apply.

Table 2 Transfer function gains

Beam current A	Zero sun		2 suns	
	J_B/J_V, dB	J_B/J_{CV}, dB	J_B/J_V, dB	J_B/J_{CV}, dB
2	7.5	2	10	-3
1	5.5	-9	4	-7
0.5	-3	-15	(a)	(a)
	$\Delta V_I/J_V$, dB	$\Delta V_I/J_{CV}$, dB	$\Delta V_I/J_V$, dB	$\Delta V_I/J_{CV}$, dB
2	34	32	29	35
1	21	30	25	27
0.5	25	23	(a)	(a)
	V_{NK}/J_{NV}, dB		V_{NK}/J_{NV}, dB	
2	22		23	
1	20		34	
0.5	33		(a)	
0.0	17		(a)	

[a]Data not taken.

E-8895

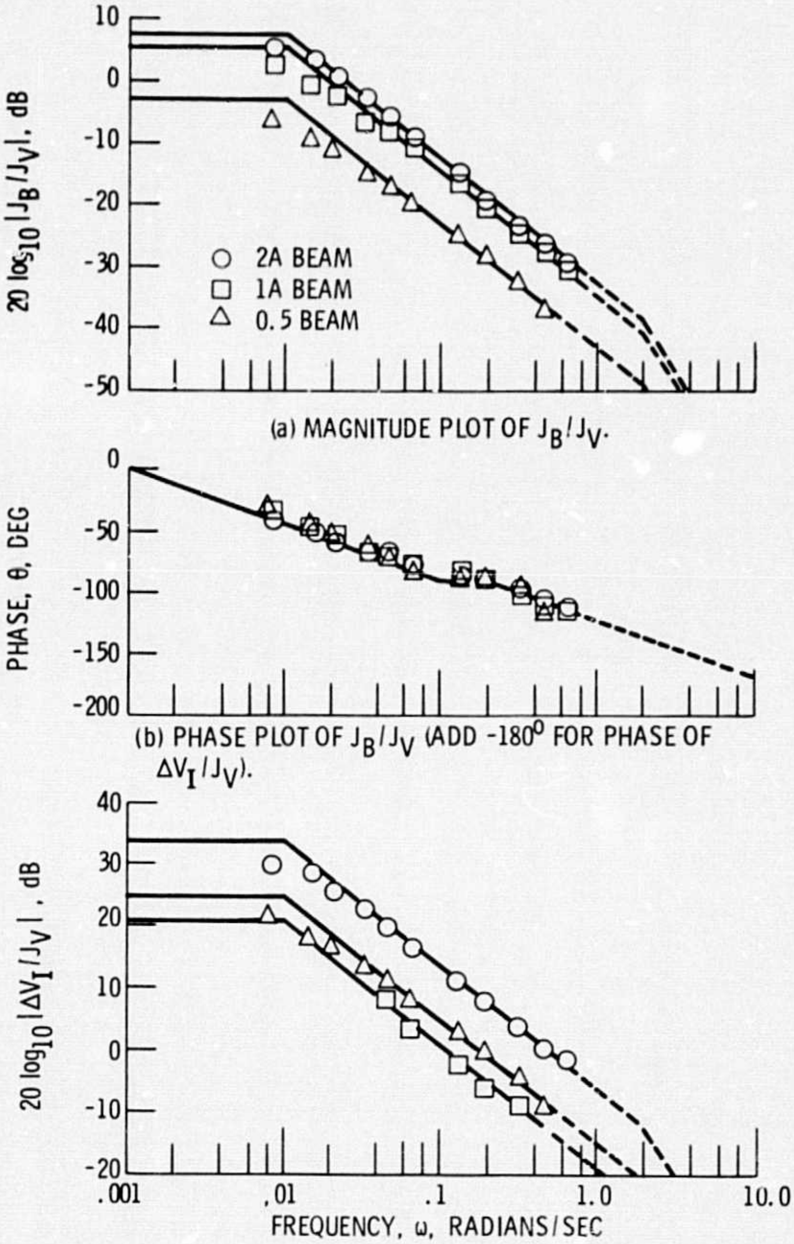

(a) MAGNITUDE PLOT OF J_B/J_V.

(b) PHASE PLOT OF J_B/J_V (ADD -180^0 FOR PHASE OF $\Delta V_I/J_V$).

(c) MAGNITUDE PLOT OF $\Delta V_I/J_V$.

Figure 1. - Response of thruster to changes in main vaporizer current at zero sun.

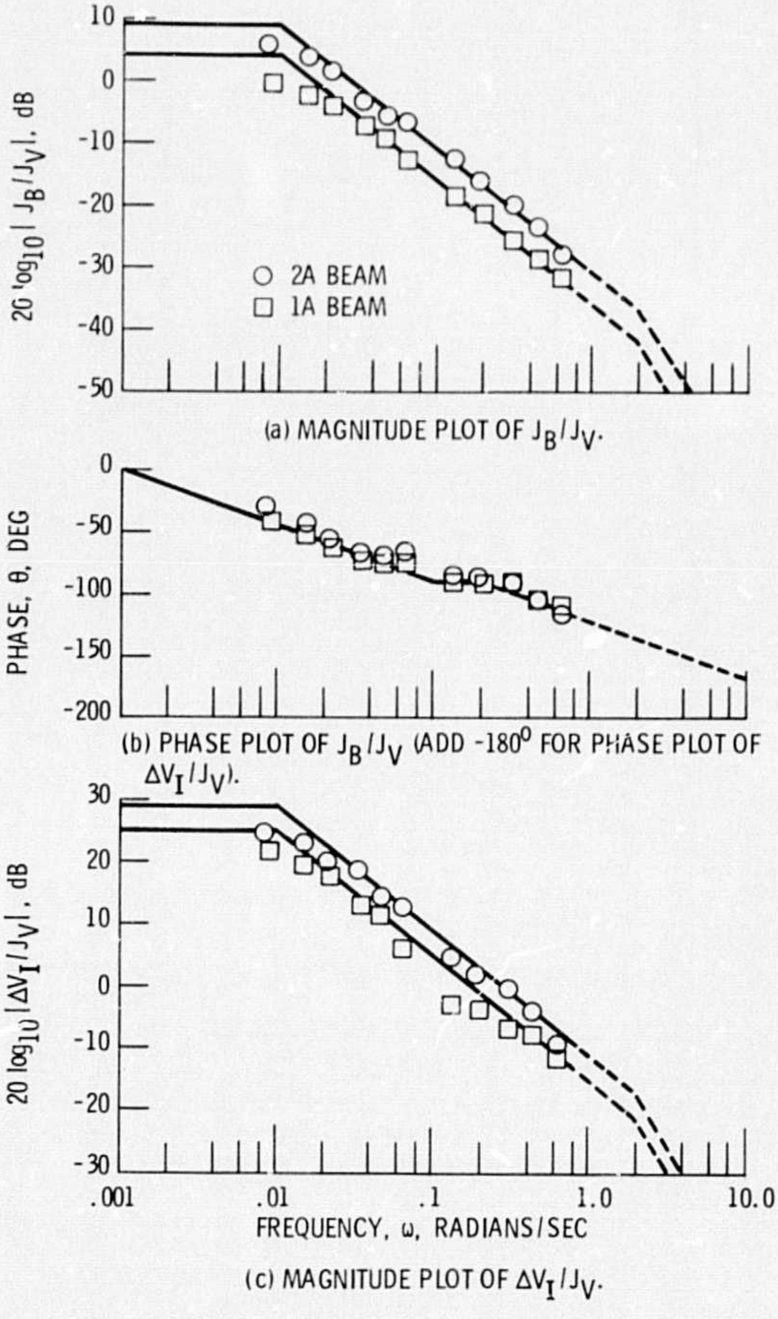

Figure 2. - Response of thruster to changes in main vaporizer current at 2 suns.

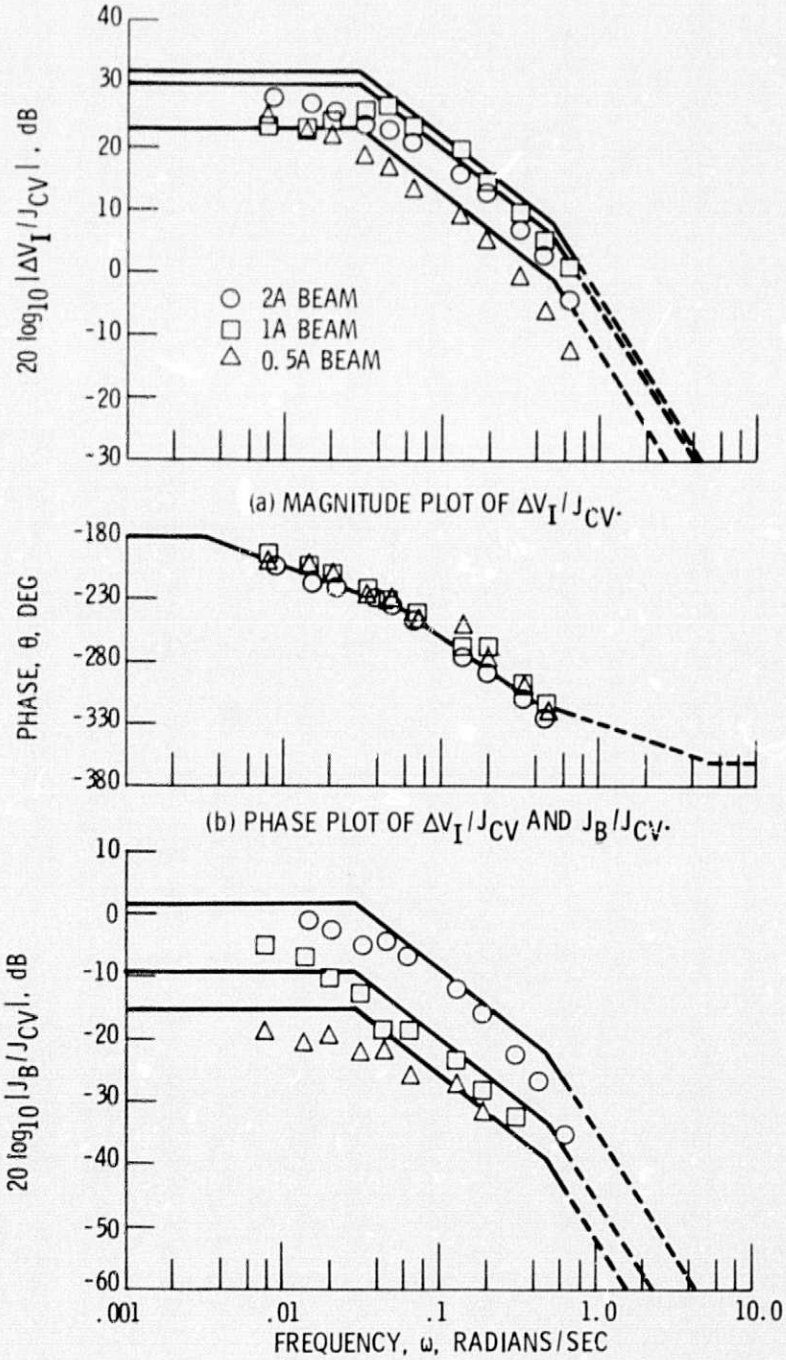

Figure 3. - Response of thruster to changes in cathode vaporizer current at zero sun.

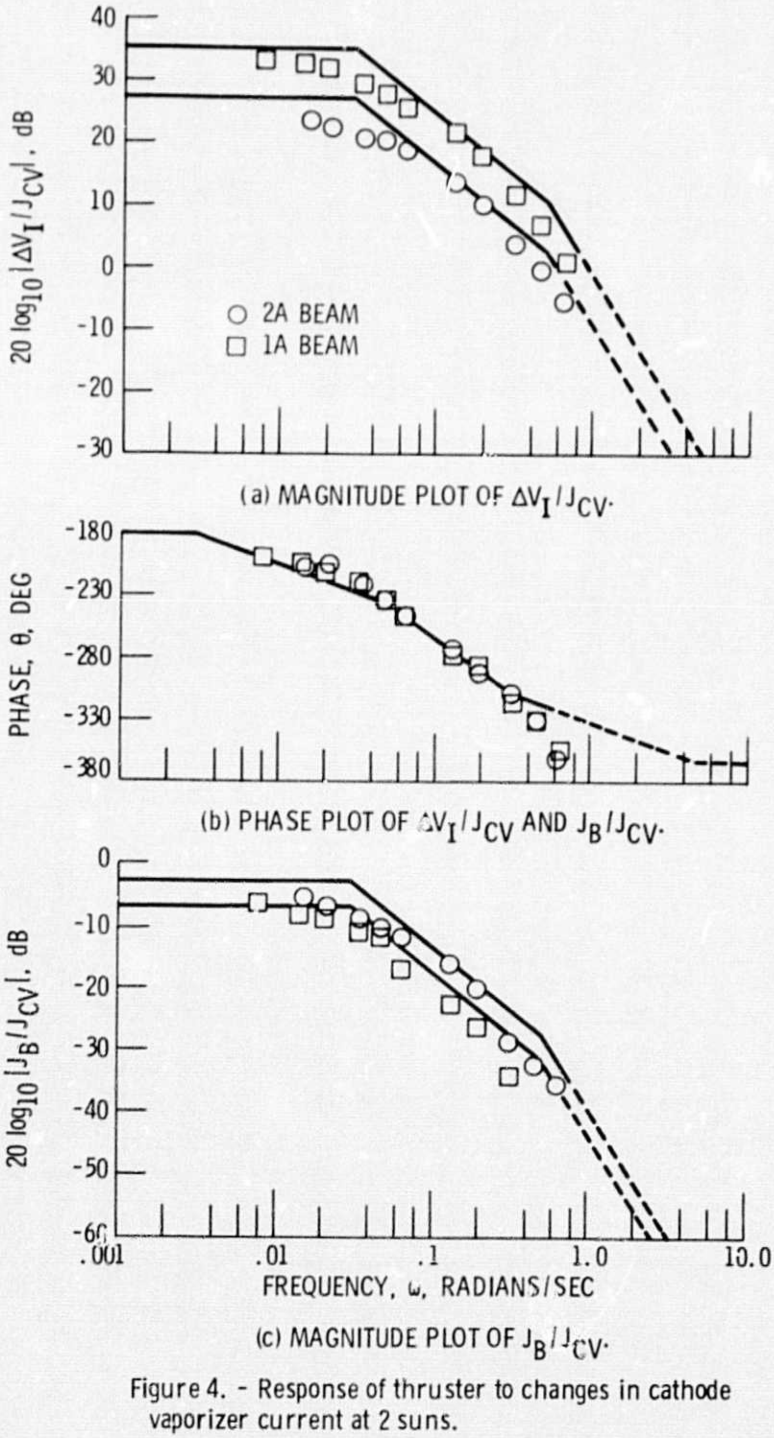

Figure 4. - Response of thruster to changes in cathode vaporizer current at 2 suns.

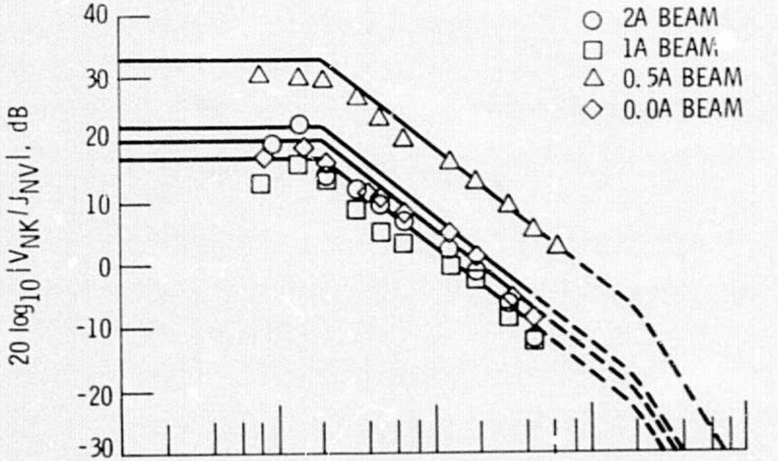

(a) MAGNITUDE PLOT OF V_{NK}/J_{NV}.

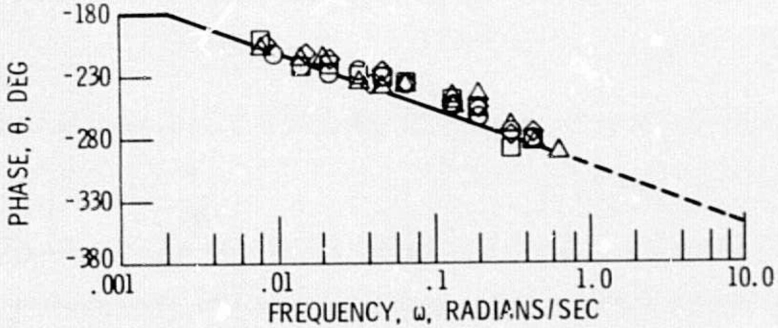

(b) PHASE PLOT OF V_{NK}/J_{NV}.

Figure 5. - Response of thruster to changes in neutralizer vaporizer current at zero sun.

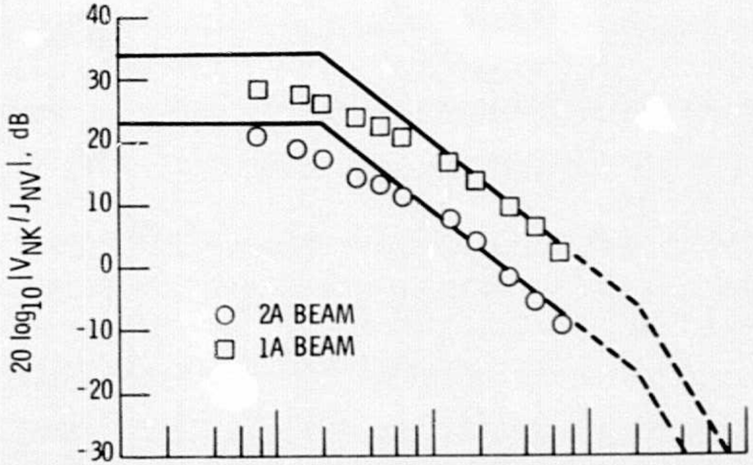

(a) MAGNITUDE PLOT OF V_{NK}/J_{NV}.

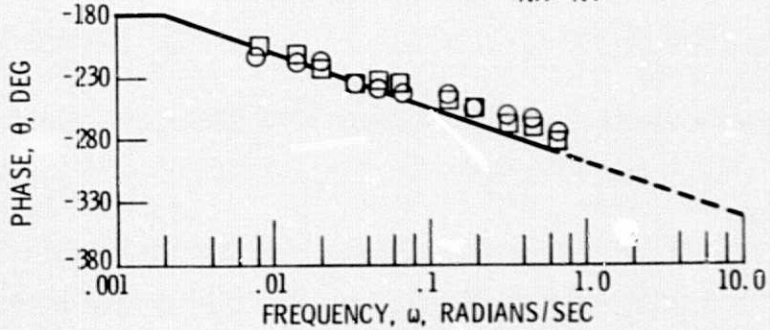

(b) PHASE PLOT OF V_{NK}/J_{NV}.

Figure 6. - Response of thruster to changes in neutralizer vaporizer current at 2 suns.

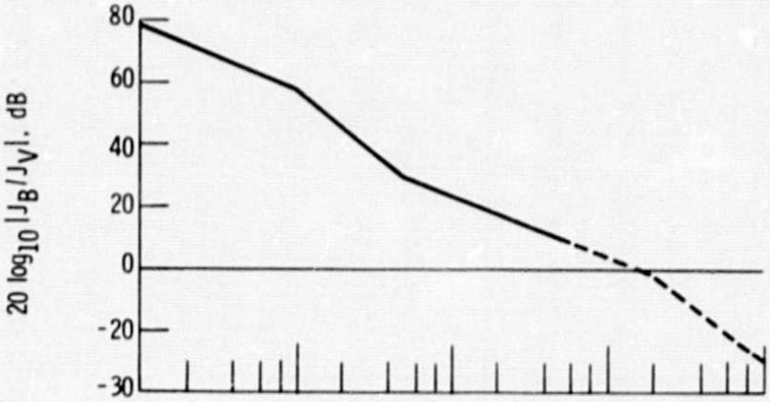

(a) MAGNITUDE PLOT OF J_B/J_V.

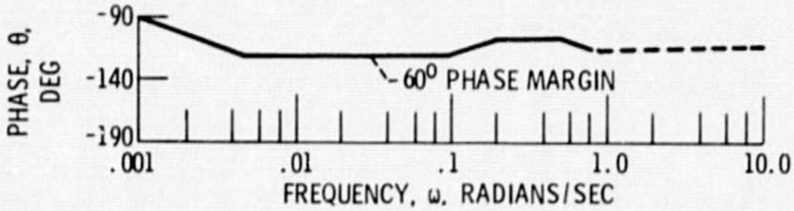

(b) PHASE PLOT OF J_B/J_V.

Figure 7. - Compensated loop for J_B/J_V. Thruster gain = 10 dB.

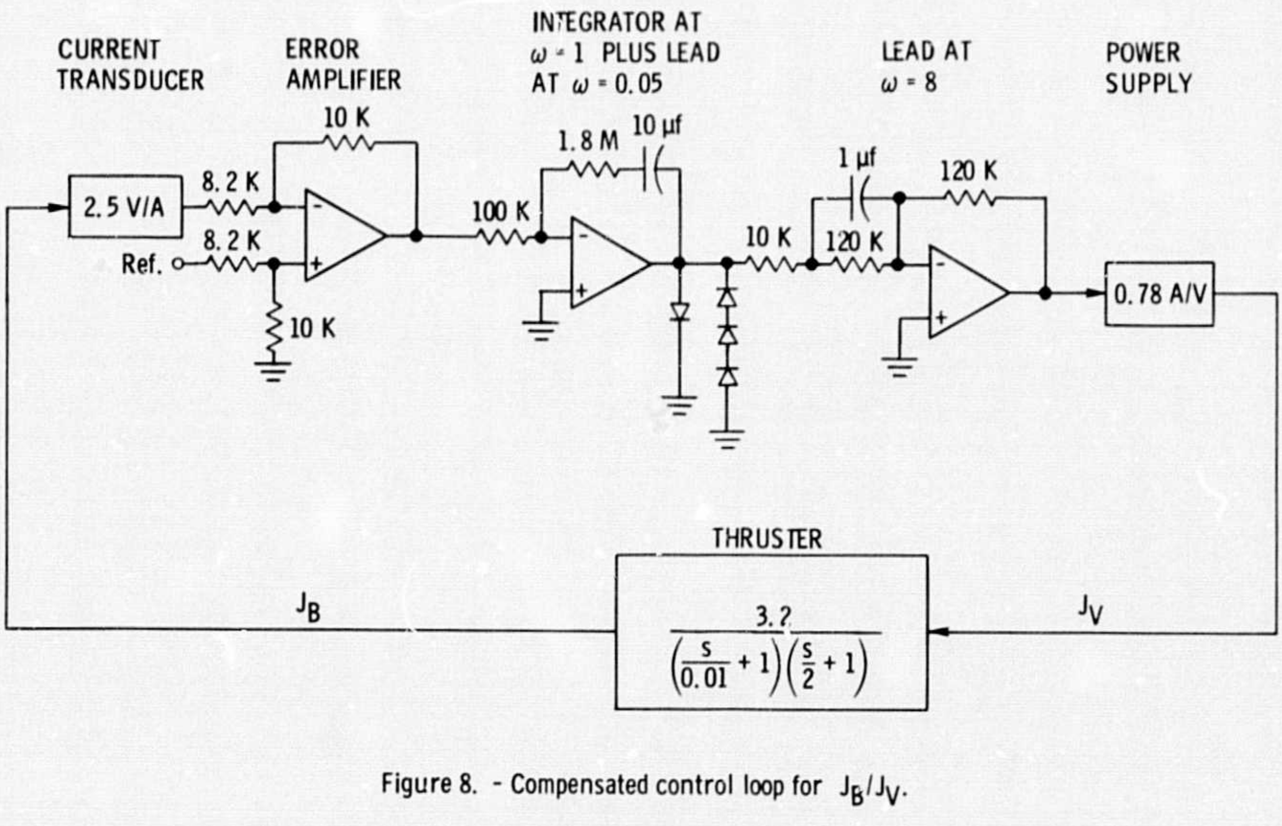

Figure 8. - Compensated control loop for J_B/J_V.

E-8895

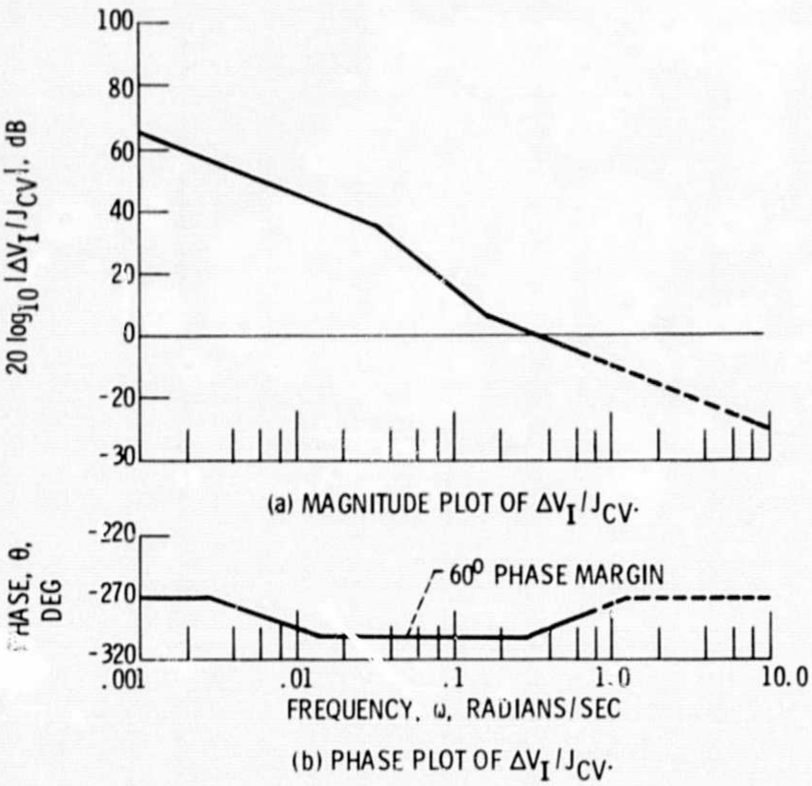

Figure 9. - Compensated loop for $\Delta V_I / J_{CV}$. Thruster gain = 35 dB.

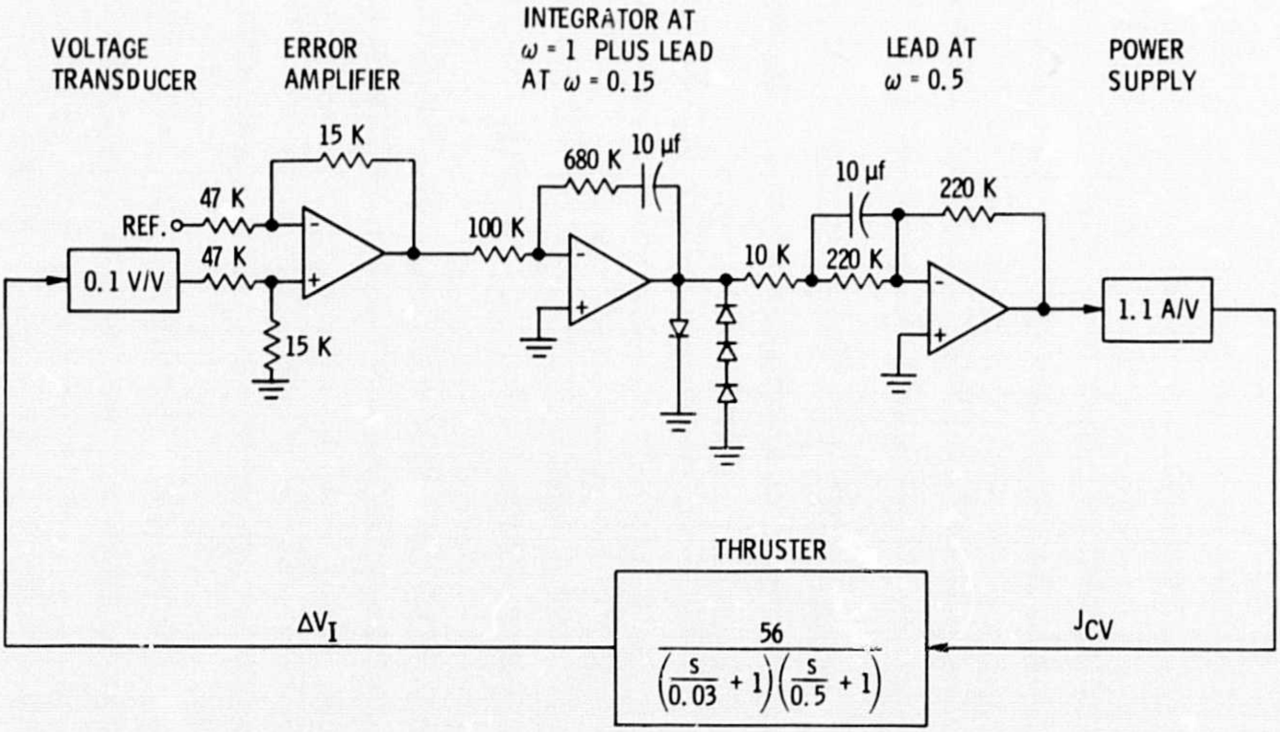

Figure 10. - Compensated control loop for $\Delta V I / J_{CV}$.

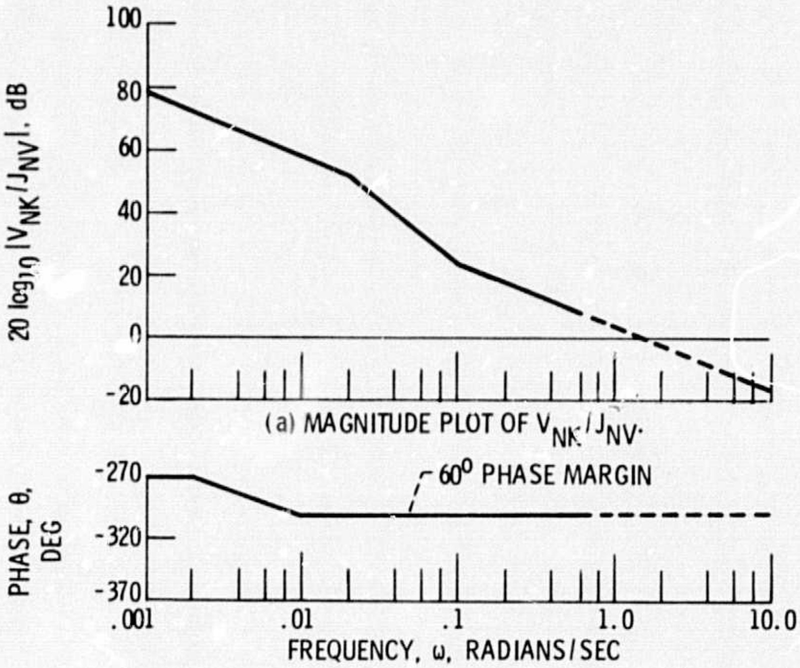

Figure 11. - Compensated loop for V_{NK}/J_{NV}. Thruster gain = 35 dB.

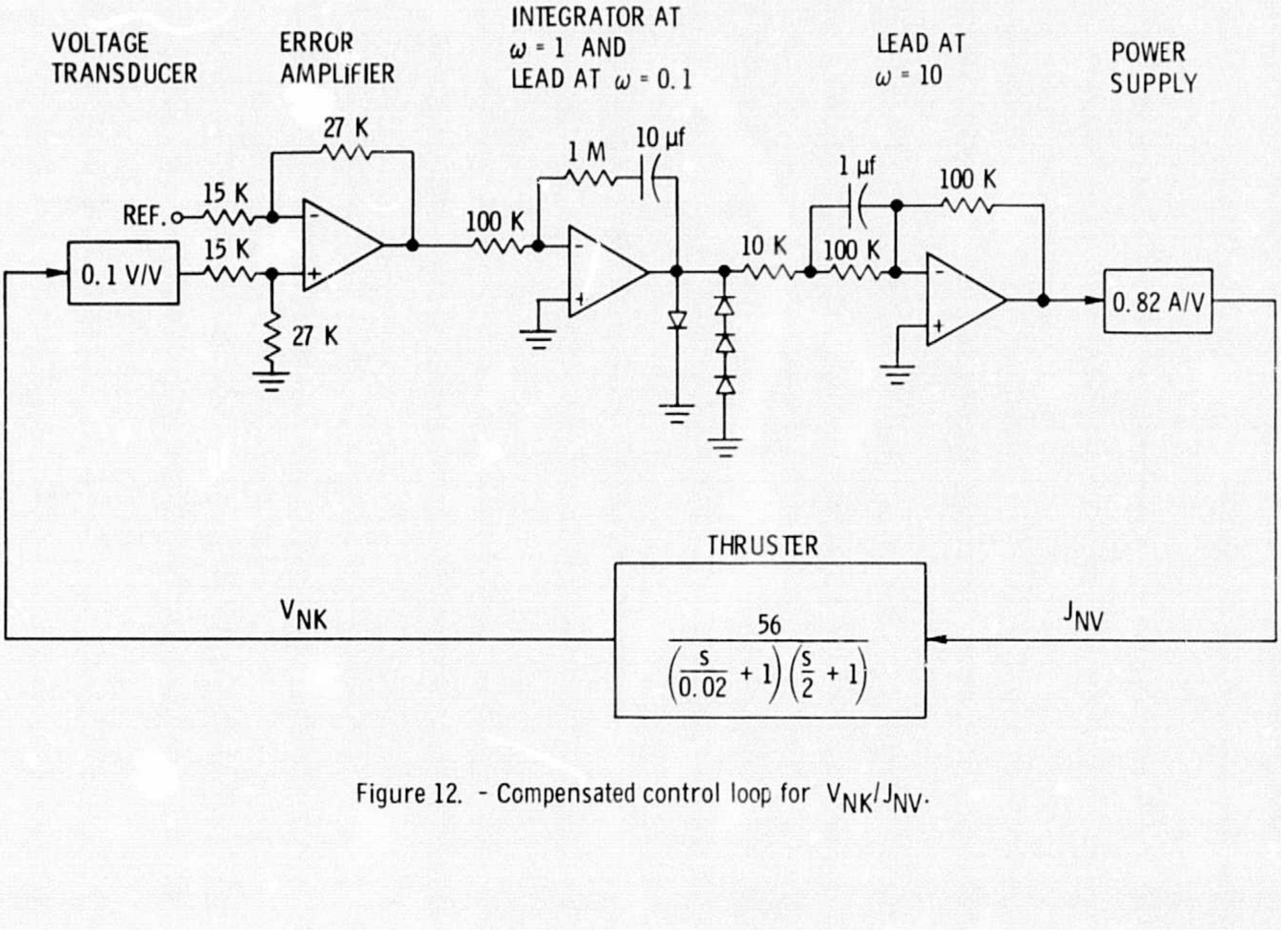

Figure 12. - Compensated control loop for V_{NK}/J_{NV}.

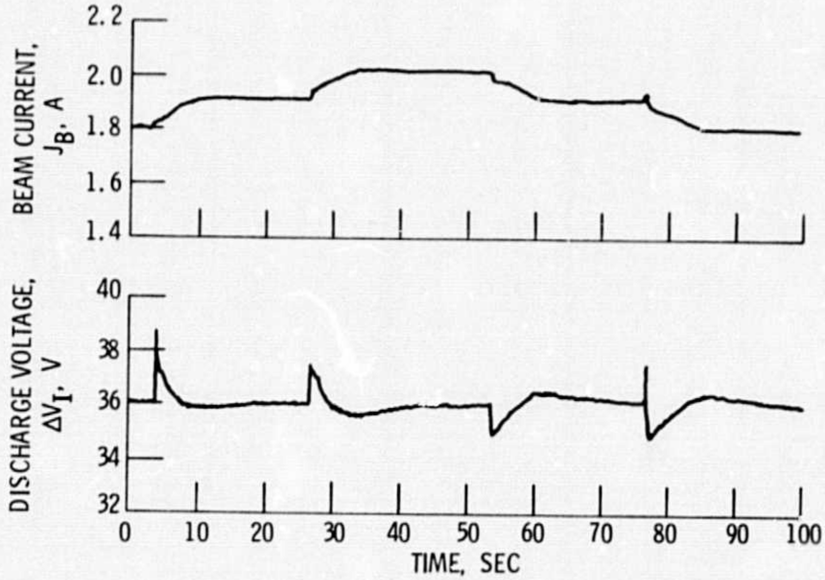

Figure 13. - Time response of beam current and discharge voltage to throttling at the 2 amp level.

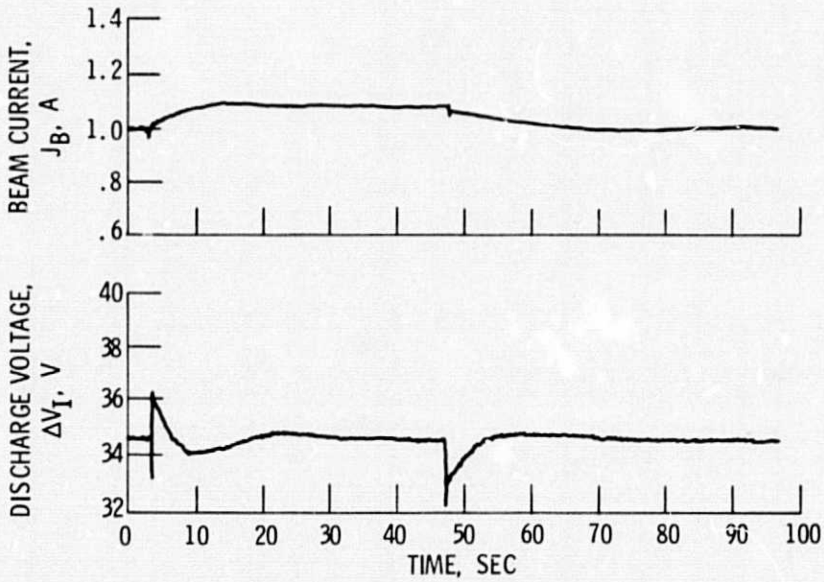

Figure 14. - Time response of beam current and discharge voltage to throttling at the 1.0 amp level.

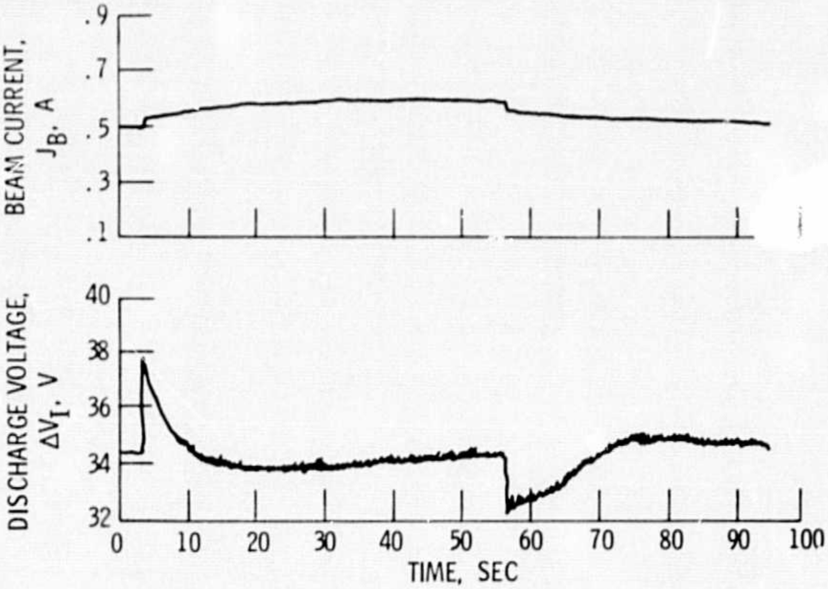

Figure 15. - Time response of beam current and discharge voltage to throttling at the 0.5 amp level.

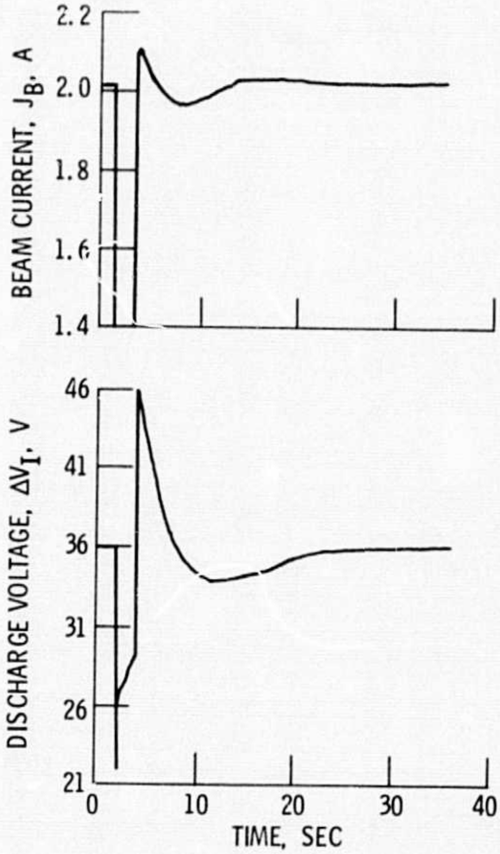

Figure 16. - Time response of beam current and discharge voltage to a recycle at the 2 amp level.

E-8895

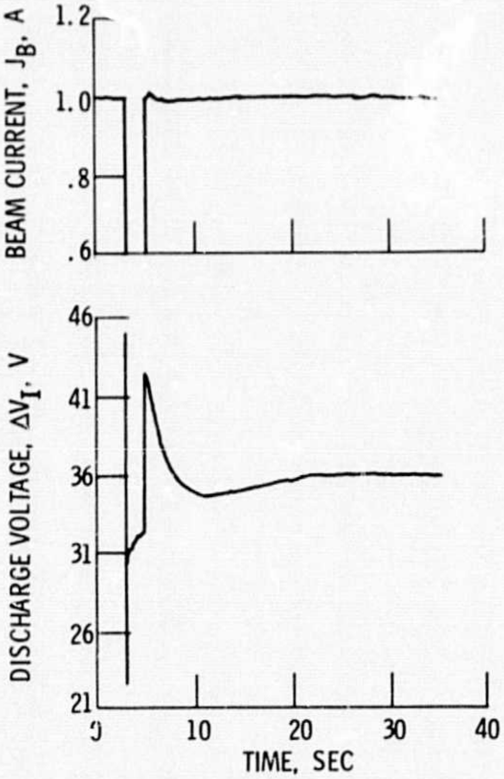

Figure 17. - Time response of beam current and discharge voltage to a recycle at the 1 amp level.

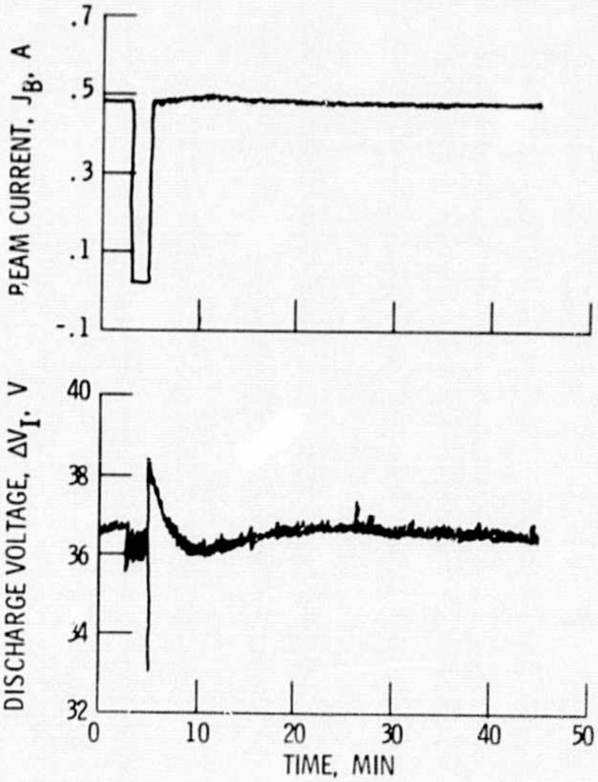

Figure 18. - Time response of beam current and discharge voltage to a recycle at the 0.5 amp level.

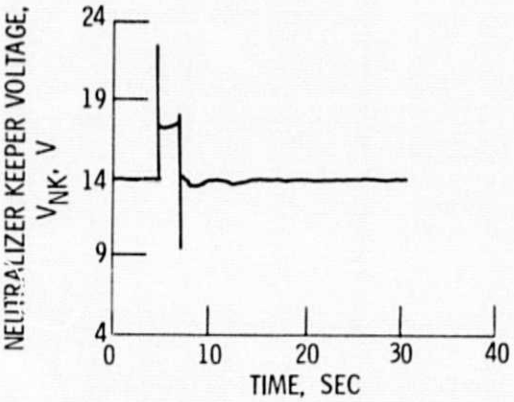

Figure 19. - Time response of neutralizer keeper voltage to a recycle at the 2 amp level.

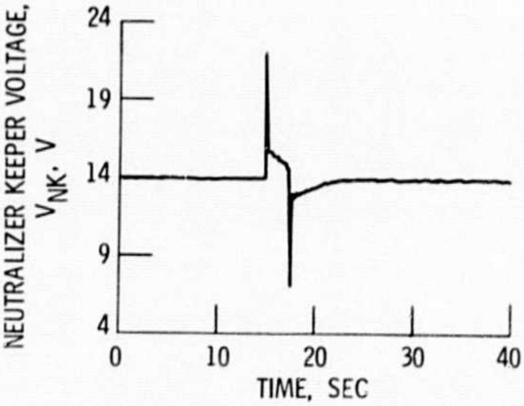

Figure 20. - Time response of neutralizer keeper voltage to a recycle at the 1 amp level.

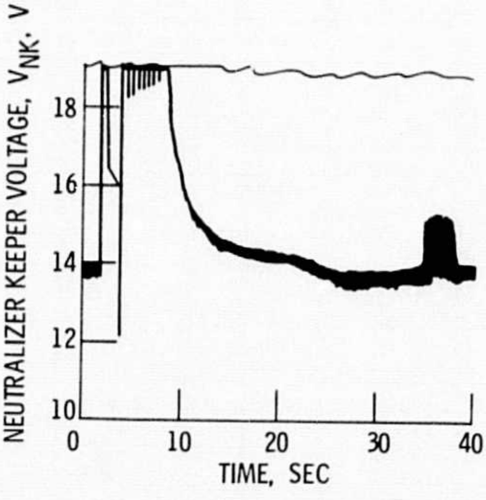

Figure 21. - Time response of neutralizer keeper voltage to a recycle at the 0.5 amp level.